

SHORT THESIS FOR THE DEGREE OF DOCTOR OF PHILOSOPHY (PhD)

# **Investigation of PARylation-dependent cell death induced by oxidative stress**

by Zsolt Regdon

Supervisor: László Virág, MD, PhD, DSc



UNIVERSITY OF DEBRECEN  
DOCTORAL SCHOOL OF MOLECULAR MEDICINE

DEBRECEN, 2021

## **Investigation of PARylation-dependent cell death induced by oxidative stress**

by **Zsolt Regdon**, Molecular Biology MSc

Supervisor: László Virág, MD, PhD, DSc

Doctoral School of Molecular Medicine University of Debrecen

Head of the **Examination Committee**: János Szöllősi, member of HAS

Members of the Examination Committee: Tamás Csont, MD, PhD

Attila Gábor Szöllősi, MD, PhD

The Examination (online format) takes place at 11 am, 12<sup>th</sup> of May, 2021.

Head of the **Defense Committee**: János Szöllősi, member of HAS

Reviewers: Ferenc Gallyas, PhD, DSc

Gábor Koncz, PhD

Members of the Defense Committee: Tamás Csont, MD, PhD

Attila Gábor Szöllősi, MD, PhD

The PhD Defense (online format) takes place at 1 pm, 12<sup>th</sup> of May, 2021.

Publicity is guaranteed during the online Defense. If you are willing to participate, please indicate via e-mail to [regdon.zsolt@med.unideb.hu](mailto:regdon.zsolt@med.unideb.hu) until 16 pm on May 11<sup>th</sup>, 2021. Due to technical reasons later sign-ups are not possible and you will not be able to join the online Defense.

## **Background**

### **The process of inflammation**

The process of inflammation has been known since ancient times. Hippocrates (around 460 BC - 377 BC) observed that the first step in the healing processes was inflammation. The Roman writer Aulus Cornelius Celsus (45 BC - 45 AD) recorded four of the five symptoms of inflammation: redness, warmth, swelling and pain. The description of the fifth symptom, the loss of function, is linked to the name of Galenos (129 BC - 200 BC). Inflammation is the immune system's response to harmful effects on the body, such as injury, pathogens and toxins. The role of inflammation is to eliminate the injury-causing agent and to initiate healing. It is characterized by increased blood flow, enhanced cellular metabolism, vasodilation, the release of mediators, oedema, and infiltration of immune cells into the inflamed area. The main phases of the inflammatory process are the recognition of the inflammatory stimulus, activation of signalling pathways, activation of transcription factors, and the release of various inflammatory mediators. These mediators elicit protective responses against pathogens, and also lead to the appearance of inflammatory markers. Neutrophil granulocytes and macrophages are the first to migrate to the site of injury. This is followed by monocytes, lymphocytes (NK, T and B cells), and mast cells. Acute inflammation is a beneficial process for the body for defending itself, while inflammation becoming chronic can lead to the development of diseases. Therefore, regulating inflammation is of paramount importance.

### **Relationship between macrophage polarization and production of ROS**

Macrophages are phagocytes and antigen presenting cells of the innate and adaptive immune systems. Macrophages can be classified into several groups based on their polarization and function. To simplify, I will discuss only the two main groups of this cell type. The inflammatory phenotype (M1) usually develops during infection or tissue injury. Polarization can be induced by bacterial lipopolysaccharide, interferon gamma, and so on. Inflammatory cytokines and chemokines are produced and a marker of this polarization is inducible nitric-oxide synthase (iNOS), which produces nitric-oxide (NO). M1 macrophages perform bactericidal, tumoricidal and phagocyte functions, however, they have been described in chronic diseases like obesity, metabolic syndrome and diabetes. The polarization of alternatively activated (M2)

macrophages can be induced by interleukin-4 (IL-4) and interleukin-10 (IL-10). M2 macrophages have immunosuppressive and angiogenic effects, and they also regulate wound healing. They are also involved in pathologic conditions such as tumor promotion, dermatitis and asthma, which are the main sources of ROS and RNS production. Under normal conditions ROS and RNS are signalling molecules, however, their overproduction leads to pathological conditions and cell death. Oxidative stress results, when the balance between the production of ROS/RNS and the antioxidant systems is disturbed. ROS/RNS can damage biomolecules (DNA, lipids, proteins) and cause cell and tissue dysfunction. Macrophages are not only producers of a high ROS/RNS environment, but also targets of oxidative stress.

### **ROS-induced cell death processes**

Oxidative stress can lead to cell death, which causes inflammation and tissue dysfunction. Apoptosis is a well characterized form of programmed cell death. Its first step is the cell's shrinkage, which is followed by the formation of apoptotic bodies, then the nucleus shrinks and fragments, and finally, the cell disintegrates into apoptotic bodies. Apoptotic bodies are ingested by phagocyte cells. Apoptosis can be induced by external (death ligands) or internal (DNA damage, ER stress, mitochondrial pathway) stimuli. Caspases are executor proteins of apoptosis. They are the members of an aspartyl protease family. We distinguish initiator (caspase-2, 8, 9, 10) and effector (caspase-3, 6, 7) caspases. Another group of caspases includes caspase-1, 4, 5, 11, 12, which are involved in the regulation of inflammation. Necrosis was originally described as a form of unregulated cell death that occurs during extreme conditions. In addition of apoptosis and necrosis, there are a number of other cell death forms. These cell death pathways usually referred to as regulated cell death, because signalling pathways are involved in their regulation. Necroptosis is a form of regulated cell death, which is phenotypically more or less similar to necrosis. Receptor-mediated signal transduction is mediated by RIPK and MLKL kinases. During necroptosis caspase-8 activation is observed, however, the cleavage of effector caspases (caspase-3) does not occur.

During ferroptosis a lethal amount of hydroxyl radical accumulates in the cell leading to a non-apoptotic cell death. Under oxidative stress, in the presence of free iron, hydroxyl radical is formed through the Fenton reaction.  $\cdot\text{OH}$  is one of the most reactive free radicals, and can damage cellular DNA, protein, and lipid molecules.

Macrophages play a crucial role in ROS/RNS production and pathogen elimination. Oxidative stress induces various forms of cell death, which can occur in macrophages, as well. To overcome this, macrophages developed a set of protective mechanisms.

### **Poly-(ADP-ribosylation)**

Mono- and poly-(ADP-ribosylation) of proteins are reversible post-translational modifications involved in the regulation of various biological processes. Just to mention a few, these are the preservation of genome stability, the regulation of transcription and cell death. According to our best knowledge, currently there are 17 members of the family. Activated PARP cleaves nicotinamide adenine dinucleotide (NAD<sup>+</sup>) to nicotinamide and ADP-ribose and synthesizes branched-chain polymers from ADP-ribose monomers to acceptor proteins.

The most intensively studied member of the PARP family is PARP-1 (also known as poly (ADP-ribose) synthetase and poly-(ADP-ribose) transferase), a nuclear protein commonly found in eukaryotes. The molecule contains three main domains: an N-terminally located DNA binding domain, an auto-modification domain and a C-terminally located catalytic domain. It also contains a nuclear localization signal (NLS) that contains the cleavage sequence of caspase-3 and a BRCT motif involved in the interaction with other proteins. The protein is highly conserved, showing 92% homology between the human and mouse amino acid sequences. The highest correspondence is found in the catalytic domain, with a 50-amino acid PARPss (PARP signature sequence) showing 100% match between different vertebrate species. PARP-1 can also interact with other PARP enzymes (PARP-1, PARP-2), DNA repair enzymes (XRCC1, DNA polymerase- $\beta$ , DNA ligase III) and other nuclear proteins such as histones and telomeric factors. DNA breakage and the consequent bending of the DNA can lead to PARP-1 activation. So can nicks. PARP activation was observed during rat primary neurons during inositol-1,4,5-triphosphate (IP<sub>3</sub>) -induced Ca<sup>2+</sup> release. PARP-1 activity is also regulated at the expression level by transcription factors Sp1 and Sp3.

PARP-1 cleaves NAD<sup>+</sup> to nicotinamide and ADP-ribose, and then covalently links ADP-ribose units to the glutamate or serine side chains of acceptor proteins. The enzyme poly-(ADP-ribose) glycohydrolase (PARG) is mainly responsible for the

removal of PAR polymers. The protein-bound ADP-ribose monomer is removed by ADP-ribosyl protein lyase.

In PARP-1 KO cells, it was found that the polymerization efficiency of short patch repair was reduced by about half, whereas long patch repair was almost completely ineffective. PARP-1 interacts with the enzyme XRCC1, which is essential in repairing SSBs. Although PARP-1 has no direct DNA repair function, it can interact with other essential enzymes of BER, such as DNA ligase III $\alpha$  and DNA polymerase  $\beta$ . There are two mechanisms for repairing double-stranded DNA breaks (DSB) in mammalian cells, homologous recombination (HDR) and non-homologous end joining (NHEJ). PARP-1 interacts with the DNA in conjunction with the XRCC1 and DNA ligase III complex when components of NHEJ are not available. It is, then, involved in error correction by creating an alternative pathway. PARP-1 is also a component of the replication complex. Its role can be thought of as a “sensor” that signals DNA damage. It helps to slow down the replication fork and allows error correction to begin.

PARP-1 also plays a prominent role in cell death. For apoptosis to occur, the amount of ATP must not fall below a certain level. The substrate for PARP enzymes is NAD<sup>+</sup>, a molecule essential for ATP synthesis. PARP-1, therefore, is a link between different cell death pathways. During apoptosis, caspase 3 proteolytically cleaves proteins and one of its substrates is PARP-1. Over-activation of PARP-1 is disadvantageous for cell survival, because it leads to ATP depletion by consuming NAD<sup>+</sup>, and results in mitochondrial dysfunction thereby inducing a necrosis-like cell death. It is clear that PARP-1 activation is essential for cell survival during genotoxicity-induced stress, however, inactivation during PCD is required for the cell to avoid the more severe form of cell death. Perhaps the most interesting form of PARP-1-mediated cell death is parthanatos. It got its name from the enzyme-catalysed reaction. (PAR refers to the poly-(ADP-ribose) polymer and Thanatos to the God of Death in Greek mythology.) It is classified as a programmed form of cell death. We distinguish it from necroptosis primarily in terms of regulation. During parthanatos, cell death is triggered by activation of PARP-1. PAR binds to AIF and induces AIF translocation from the mitochondria to the nucleus. However, translocation of AIF does not explain fragmentation in the nucleus. The nuclease MIF is responsible for DNA cleavage. We can see that PARP-1 plays an important role in the regulation of cell death.

## **Aims**

The PARP-1 enzyme plays a significant role in DNA repair, transcriptional regulation, and cell death. In addition, PARP-1 plays a central role in the regulation of inflammatory processes in immune cells. While there is extensive literature about the mechanisms of DNA repair and PARP-1-mediated cell death, little is known about the role of PARP-1 in the development of resistance of macrophages to oxidative stress. Therefore, we set the following goals for our work:

- 1) To investigate the sensitivity of macrophages of different polarization states to H<sub>2</sub>O<sub>2</sub>.
- 2) To determine the gene expression profile of H<sub>2</sub>O<sub>2</sub>-resistant M1 macrophages.
- 3) To identify the role of PARP-1 in the development of H<sub>2</sub>O<sub>2</sub> resistance in M1 macrophages.
- 4) To characterize the metabolism of M1 macrophages under oxidative stress.

The repurposing of drugs already marketed as medicines for use in other diseases has a great importance in drug research. PARP-1 plays an important role in the regulation of cell death, therefore we aimed to explore molecules that may play a role in parthanatos suppression. Our specific goals related to this aim were:

- 1) To set up a HCS method for the identification of cytoprotective molecules.
- 2) To perform screening on a small molecule library (<800) and validate “hit” compounds.
- 3) To identify PARP inhibitors.
- 4) To characterize their mechanism of action.

## Materials and methods

### Materials

3- (4,5-dimethylthiazol-2-yl) -2,5-diphenyltetrazolium bromide (MTT), low melting point agarose (LM agarose), antimycin, apomorphine, ciclopirox, Dulbecco's Modified Eagle's Medium (DMEM), fetal bovine serum (FBS), H<sub>2</sub>O<sub>2</sub>, interleukin-4 (IL-4) carbonyl cyanide-4- (trifluoromethoxy) phenylhydrazone (FCCP), lipopolysaccharide (LPS), NAD / NADH Quantitation Kit, oligomycin, propidium iodide (PI), protease inhibitor cocktail (PIC), RPMI-1640 medium was obtained from Sigma-Aldrich Kft (Budapest, Hungary). L-glutamine and penicillin / streptomycin are from Lonza Group AG (Basel, Switzerland). DMEM medium used for Seahorse experiments was obtained from Agilent (Santa Clara, CA, USA). FITC Annexin V Apoptosis Detection Kit I was purchased from BD Pharmingen (San Jose, CA, USA). The following antibodies: anti-AIF antibody, anti-PARP-1 antibody, HRP-conjugated anti-mouse IgG, HRP-conjugated anti-rabbit IgG from Cell Signaling Technologies (Danvers, MA, USA), peroxidase-conjugated and anti- $\beta$ -actin antibody was purchased from Santa Cruz Biotechnology (Dallas, TX, USA). Anti-phospho-H2AX antibody was obtained from Trevigen (Minneapolis, MN, USA). The monoclonal anti-PAR antibody was purified from the supernatant of 10 H hybridoma cells prepared at the Institute of Medical Chemistry of the University of Debrecen with a saturated ammonium sulfate solution. The skim milk powder used to block the membranes was commercially available. The K4 transfection system was obtained from Biontex Laboratories (Munich, Germany). The PARP1-mCherry OmicsLink expression plasmid was obtained from GeneCopoeia (Rockville, MD, USA). The ATP A Screen-Well® FDA Approved Drug Library V2 molecule library was purchased from Enzo Life Sciences Inc. (Farmingdale, NY, USA). 4',6-diamidino-2-phenylindole (DAPI), Hoechst 33342, and Sytox Green are from Invitrogen (Carlsbad, CA, USA). Reagents for qPCR were obtained from the following companies: Trizol reagent was purchased from the Molecular Research Center (Cincinnati, OH, USA). The High Capacity cDNA Reverse Transcription Kit was purchased from Applied Biosystems (Foster City, CA, USA) and the 2X qPCRBIO Sygreen Mix Lo-ROX reagent was purchased from PCR Biosystems (London, UK). Recombinant mouse macrophage colony stimulating factor (M-CSF) was purchased from R&D System (Minneapolis, MN, USA). The ATP Bioluminescence Assay Kit II is from Roche Diagnostics (Penzberg, Germany). Hank's



Balanced Saline (HBSS), Lipofectamine 3000 and SuperSignal <sup>TM</sup> West Pico PLUS Chemiluminescent Substrate are from Thermo Fisher Scientific (Vantaa, Finland). The following reagents were purchased from VWR International Kft (Debrecen, Hungary): dimethyl sulfoxide (DMSO), phenylmethylsulfonyl fluoride (PMSF), glycerol, mercaptoethanol, sodium dodecyl sulfate (SDS), sodium hydroxide, Na<sub>2</sub>EDTA, TrisHCl, Triton X-100.

## **Methods**

### *Isolation, differentiation, and polarization of bone marrow-derived macrophages (BMDM)*

Bone marrow cells from C57 mice (University of Debrecen Life Sciences Building Experimental Animal House) were isolated as described in I Pineda-Torra et al., 2015. The protocol for the collection of mouse bone marrow macrophages was in accordance with the Declaration of Helsinki and approved by the Regional Research Ethics Committee (15/2016 / DEMÁB). BMDM cells were incubated in DMEM (differentiating medium) supplemented with 10% heat-inactivated FBS, 1% L-glutamine, 1% penicillin streptomycin, and 25 ng / ml mouse M-CSF. The cells were maintained at 37 ° C and 5% CO<sub>2</sub>. Fresh differentiation medium was added to the cell culture on days 3 and 5. On day 6, cells were considered as fully differentiated macrophages. Cells were treated with 10 ng / ml LPS or 5 ng / ml IL-4 to induce M1 or M2 polarization respectively.

### *HaCaT cell culture*

HaCaT cells (SigmaAldrich, St. Louis, MO, USA) were cultured in RPMI 1640 supplemented with 10% FBS, 1% L-glutamine and 50 U / ml / 50 µg / ml penicillin / streptomycin solution at 37 ° C in an atmosphere containing 5% CO<sub>2</sub>.

### *Cell viability assay (MTT assay)*

Cell viability was measured by MTT assay. 0.5 mg / ml MTT solution was added to the cells and incubated for 30 minutes. The medium was aspirated and the formazan crystals were dissolved in 100 µl DMSO. Absorbance was measured at 590 nm on a Tecan Spark photometric instrument (Tecan Group Ltd., Männedorf, Switzerland). Viability was calculated and expressed as a percentage of control.

### *Evaluation of cell confluence and propidium iodide uptake*

Confluence was measured in representative images taken with the imaging function of the Tecan Spark plate reader. For PI uptake assays, cells were incubated with 5 µg / ml PI for 15 min. Fluorescence intensity was measured at 560 ex / 620 em with a Tecan Spark plate reader.

### *High content analysis of cell death (HCA)*

For all HCA experiments, cells were cultured on CellCarrier Ultra plates (Perkin Elmer, Ealtham, MA, USA). After staining, images were taken with Opera Phenix HCS (Perkin Elmer, Ealtham, MA, USA) and data were analyzed with Harmony software (Perkin Elmer, Ealtham, MA, USA).

### *Annexin V-propidium iodide double staining*

After treatment, cells were washed with PBS and stained vitally with Hoechst and FITC Annexin V Apoptosis Detection Kit I according to the manufacturer's instructions. Images were taken with a 10x air objectives. Nuclear and cytoplasmic regions were segmented based on Hoechst intensity. Mean fluorescence intensity (MFI) was calculated for the FITC cell area and for PI in the nucleus area. Based on MFI, three cell subgroups were identified: living (double negative), apoptotic (Annexin V - FITC positive, and PI negative), and necrotic (PI positive) cells.

### *RNA isolation, reverse transcription, and quantitative real-time PCR*

Total RNA isolation was performed by the Trizol method. 2 µg of RNA was used for reverse transcription, transcription was performed with a high capacity High Capacity cDNA Reverse Transcription Kit according to the manufacturer's instructions. Real-time quantitative PCR was performed using a 2X qPCRBIO Sygreen Mix Lo-ROX and a Roche Lightcycler 480II (Roche Diagnostics GmbH, Penzberg, Germany).

### *SDS-PAGE and Western blot*

For size separation of proteins in cold lysis buffer (62.5 mM Tris-HCl (pH 6.8), 2% SDS, 10% glycerol, 715 mM 2-mercaptoethanol, 1 mM PMSF (phenylmethylsulfonyl fluoride), protease inhibitor cocktail) were run on an 8% SDS-polyacrylamide gel and subjected to polyacrylamide electrophoresis (PAGE) at 100 V for 90 minutes. Proteins were transferred to a nitrocellulose membrane at a current of 400 mA for 90 min.

Membranes were blocked with a solution of 5% skim milk powder in 1X PBST buffer for 1 hour at room temperature. Membranes were incubated with antibodies to PAR (clone 10H), PARP-1, and  $\beta$ -actin overnight at 4 °C. The next day, the membranes were incubated in HRP-conjugated secondary antibodies for 2 hours at room temperature, according to the primary antibodies. Between steps, the membrane was washed twice with 1X PBST for 5 min and then in 1X PBS buffer for 5 min. Antibody binding was detected by chemiluminescence using the Chemidoc Touch gel documentation system (Bio-Rad Laboratories Irvine, CA, USA) SuperSignal™ West Pico Chemiluminescent Reagent.

#### *NAD<sup>+</sup> and ATP assay*

Relative NAD<sup>+</sup> content was determined with the NAD / NADH Quantitation Kit according to the manufacturer's instructions. Absorbance was normalized to protein content. Relative ATP content was determined with the ATP Bioluminescence Assay Kit II according to the manufacturer's instructions. ATP content was normalized to protein content. Measurements were done on a Tecan Spark plate reader (Tecan, Männedorf, Switzerland).

#### *Measurement of extracellular acidification and oxygen consumption rate*

Mouse bone marrow cells were differentiated on a Seahorse XF96 (Agilent Technologies, Santa Clara, CA, USA) cell culture plate and then treated as described in the results. After aspirating the medium, cells were incubated for 1 hour in XF assay medium-modified DMEM (pH 7.4) supplemented with 4.5 g / l glucose. Oxygen uptake rate (OCR) and extracellular acidification rate (ECAR) were determined with an XF96 extracellular flux analyser (Agilent Technologies, Santa Clara, CA, USA). Mitochondrial stress test was performed by sequential addition of oligomycin (2  $\mu$ M), FCCP (4  $\mu$ M), and antimycin (10  $\mu$ M). After the addition of each compound, the OCR was measured four times (5 min / measurement). Secondary metabolic parameters (ATP-bound respiration, maximal respiratory capacity, respiratory reserve capacity) were determined by Dranka et al. calculated as described in the publication (B P Dranka et al., 2011).

### *Analysis of thymocyte cell death by flow cytometry*

Thymocyte isolation was performed according to Hegedűs et al. (C Hegedűs et al., 2008). C57 / Bl6 mice (University of Debrecen Life Science Building Experimental Animal House) were terminated at 4-6 weeks of age, then the thymus was aseptically dissected, placed in ice-cold RPMI 1640 medium, and prepared on a stainless steel wire mesh screen with a 100 µm nylon screen. Thymocytes were diluted to a density of  $2 \times 10^6$  / ml with RPMI 1640 medium, then 100 µl was placed in a 96-well plate. Following treatment, cells were stained with 1.25 µg / ml PI for 5 min and cell death was measured with an Acea NovoCyte (Agilent Technologies, Santa Clara, CA, USA) flow cytometer.

### *Transfection of PARP1-mCherry into HaCaT cells*

The expression plasmid PARP1-mCherry OmicsLink was used for transfection. HaCaT cells were placed in ibidi 8-well µ-chambers (ibidi GmbH, Gräfelfing, Germany) the previous day. Two hours before transfection, cells were treated with K4 multiplication reagent from the K4 transfection system and incubated with plasmid DNA (300 ng / well) mixed with Lipofectamine 3000 at a ratio of 1: 1 µg / µl. The medium was changed 5 hours later to normal medium containing 1/200 K4 multiplier. Cells were used for a microirradiation experiment 36-48 hours later.

### *Microirradiation and image analysis*

Laser microirradiation (IR) was performed with a Leica TCS SP8 confocal microscope (Leica Microsystems, Wetzlar, Germany) using the FRAP module of the LAS X software. HaCaT cells were incubated with 10 µg / ml Hoechst 33342, and then the medium was changed to FluoroBright containing test compounds without Hoechst. Images were taken with a Leica HC PL Apo CS 40x / NA 0.85 dry objective through a 99.94 µm diameter hole with an optical slice thickness of 1.6 µm. The zoom factor was set to 2x and frames were taken with 400 Hz bidirectional scanning at 1024x256 px digital resolution. A 552 nm OPSL laser was used to excite the mCherry. For microirradiation of PARP1-mCherry transfected cells, a 0.4 mW 405 nm diode laser was set at 3.5% power and irradiated for 2 seconds at a point in the nucleus using the LAS X PointBleach function. Forty pre-irradiation images were collected every 328 ms. After IR, 200 images were taken with the settings used in the pre-irradiation period.

### *Immunofluorescent staining and fluorescence microscopy*

HaCaT cells were cultured in Cell Carrier Ultra plates (PerkinElmer, Waltham, MA, USA). Cells were treated as described in figure legend, after washing with PBS buffer, fixed with methanol for 20 min at -20 °C for PAR polymer (10H clone) and PARP-1 antibodies, or fixed in 4% PFA at room temperature for 15 min for AIF and  $\gamma$ H2AX staining. The cells were then washed three times with PBS, permeabilized in PBS containing 0.5% Triton-X for 5 minutes, and blocked with PBS containing 1% BSA for 60 minutes. Cells were incubated with primary antibodies diluted in blocking solution overnight at 4 °C with gentle shaking. After washing three times with PBS, the cells were incubated for 45 min with the secondary antibody and DAPI (2  $\mu$ g / ml) in PBS. Cells were washed three times with PBS and kept in PBS until fluorescence microscopy. Imaging was performed with Opera Phenix (Perkin Elmer, Waltham, MA, USA). All image analyses were performed with Harmony software (Perkin Elmer, Waltham, MA, USA).

### *Comet assay*

The alkaline comet assay was performed using Trevigen FLARE™ slides (Trevigen, Gaithersburg, MD, USA) according to the manufacturer's instructions with some modifications as follows: following trypsin treatment,  $10^5$  HaCat cells were pretreated with DMSO (vehicle), apomorphine (10  $\mu$ M), or ciclopirox (10  $\mu$ M) for 1 h. Cells were treated with H<sub>2</sub>O<sub>2</sub> at a final concentration of 200  $\mu$ M for 10 min. The cells were then centrifuged at 4 °C and suspended in 1 ml of ice-cold PBS. To the cell suspension (40  $\mu$ l), 400  $\mu$ l of molten LM agarose (1%, 37 °C) was added, and 40  $\mu$ l of the cell suspension-agarose mixture was immediately pipetted onto a Trevigen FLARE™ slide. Slides were kept in the dark at 4 °C for 30 minutes and then immersed in cold Lysis Solution (Trevigen, Gaithersburg, MD, USA). After overnight lysis, slides were incubated for 3 x 30 minutes at room temperature in electrophoresis buffer (0.03 M NaOH, 2 mM Na<sub>2</sub> EDTA, pH 12.3). Electrophoresis was performed at 4 °C for 30 minutes at 20 V. After rinsing the slide in distilled water and neutralizing, the nuclei were stained with 10  $\mu$ g / ml PI for 30 minutes. After washing with distilled water, the slides were dried at room temperature to place the cells on the same plane. Prior to analysis, a thin layer of molten 1% LM agarose was pipetted onto slides to reduce

background fluorescence. Images were taken with a Leica SP8 Confocal microscope. Images were analysed with Open Comet software.

#### *PARP1 chromatin binding assay (PARP1 trapping assay)*

HaCaT cells were cultured in Cell Carrier Ultra plates (Perkin Elmer, Waltham, MA, USA). Cells were treated as described in the figures. Cells were then extracted on ice in 0.2% Triton X-100 for 2 minutes, fixed with methanol at -20 ° C, and stained with PARP1 antibody according to Michalena et al. as described in the publication (J Michelena et al. 2018).

#### *Calcein dequenching assay (detection of intracellular iron chelation)*

HaCat cells were incubated with 250 nM calcein-AM for one hour. Cells were washed twice with HBSS containing 0.4 mM calcium and magnesium and incubated for 30 min to allow uncleaved calcein-AM to diffuse from the cells. The medium was changed to HBSS containing 2.5 µg / ml PI, and the cells were incubated for an additional 30 min to equilibrate the PI between the medium and the cell interior. Both calcein and PI fluorescence were recorded kinetically. The recording consisted of three stages. After an initial equilibration period of 15 min, 10 µM ciclopirox or apomorphine was injected into the designated wells using the instrument injector pump. Subsequently, the reduction of calcein fluorescence was followed for 30 min. Finally, a third phase in which 200 µM H<sub>2</sub>O<sub>2</sub> was injected into the designated wells and its effect on the intracellular labile iron pool was observed as a change in calcein fluorescence for 45 min.

#### *Statistical analysis*

Primary data were averaged by the standard deviation of 3-5 independent experiments. Statistical analysis was performed using GraphPad Prism 8 as described in the Results section. Chapter is shown in the signatures. P values below 0.05 were considered significant.

## **Results**

### **The role of PARP-1 in resistance development against oxidative stress in polarized macrophages**

#### **M1 macrophages have increased resistance against H<sub>2</sub>O<sub>2</sub>**

First, we determined the H<sub>2</sub>O<sub>2</sub> concentration required to induce cell death. Macrophages showed a high degree of resistance to cell death. Based on the MTT assay 1 mM H<sub>2</sub>O<sub>2</sub> was needed to cause cell death. This concentration was used in the following experiments. To determine if there was a difference in H<sub>2</sub>O<sub>2</sub> sensitivity of macrophages of different polarization, BMDM cells were pretreated with LPS and IL-4 for 24 h. Then, the cells were treated with H<sub>2</sub>O<sub>2</sub> and their viability was measured. M1 macrophages showed resistance to H<sub>2</sub>O<sub>2</sub>. The LPS-induced protection from cell death was measured by a cell permeability assay (PI uptake). Cell condensation was also analysed in H<sub>2</sub>O<sub>2</sub> treated cells, and we found that it was suppressed by LPS pretreatment. We also performed Annexin V and PI double staining on the treated cells. We did not find Annexin V single positive cells, so the occurrence of apoptotic cell death was excluded.

#### **Expression changes in cell death regulatory and antioxidant genes during M1 polarization**

To explore the anti-necrotic effect of LPS, we designed qPCR assays to determine the expression of cell death and antioxidant genes. Markers of apoptosis (Bak1 and Casp3) were unchanged, whereas markers of parthanatos (Parp1 and Aif) were significantly decreased. Parp-1 expression was also decreased at the protein level, which was confirmed by Western blot. While we measured catalase that directly catalyses the elimination of H<sub>2</sub>O<sub>2</sub>, we also determined NADH/GSH-linked enzymes (Txnrd1, Prxd1, Gsr) and superoxide dismutases (Sod1 and Sod2) responsible for secondary superoxide removal. Catalase expression was decreased by LPS, the same was true for Sod1. The expression of Txnrd1, Prxd1 and Gsr was significantly increased, the largest increase was observed in the expression of Sod2.

#### **Decreased PARylation and maintained NAD<sup>+</sup> levels in M1 macrophages**

PARP-1 activity was performed by detecting the PAR polymer. Upon H<sub>2</sub>O<sub>2</sub> treatment there was no detectable amount of PAR in PARP-1 KO BMDM cells, thus

confirming that PARP-1 is responsible for PARylation. M1 macrophages showed decreased PARylation. Hyper-activation of PARP-1 leads to  $\text{NAD}^+$  depletion. The intracellular  $\text{NAD}^+$  level decreased almost to zero in  $\text{H}_2\text{O}_2$  treated cells, while in PARP-1 KO and LPS-pretreated cells its level was significantly higher. To confirm that PARP-1 is responsible for mediating cell death, a PI assay was performed. The appearance of a necrotic population upon  $\text{H}_2\text{O}_2$  treatment was delayed in PARP-1 KO cells. However, LPS-pretreated cells were resistant to  $\text{H}_2\text{O}_2$ , so we hypothesized that other mechanisms might be involved in the development of resistance.

### **AIF-independent parthanatos inhibition in M1 macrophages**

Nuclear condensation is a marker of parthanatos. As confirmed by fluorescent microscopy nuclear condensation was inhibited by LPS and PJ34 pretreatment. Another canonical marker of parthanatos is the translocation of AIF from the mitochondria to the nucleus. Confocal microscopy failed to confirm the nuclear presence of the AIF, so we can speak of an AIF-independent parthanatos.

### **Metabolism of M1 macrophages shifts toward aerobic glycolysis, while mitochondrial activity decreases and ATP levels are maintained**

Upon  $\text{H}_2\text{O}_2$  treatment mitochondrial dysfunction and the inability of ATP synthesis occur. Seahorse analysis was performed to measure the metabolic status of the cells. Basal respiration was significantly reduced by  $\text{H}_2\text{O}_2$  treatment, which was unaffected by LPS and PJ34 pretreatment. The same was true for ATP-linked mitochondrial activity. The most drastic decreases were measured in the maximal respiratory and reserve capacities after  $\text{H}_2\text{O}_2$  treatment. PJ34 rescued the decreases of both. LPS pretreatment already drastically reduced these parameters in the control cells, so it could not counteract the effect of  $\text{H}_2\text{O}_2$  treatment in the same way as PARP inhibition did. On the other hand, LPS pretreatment significantly increased glycolysis and the proton production rate. An ATP assay was used to measure the intracellular ATP levels. LPS and PJ34-pretreated cells showed significantly higher ATP levels compared to  $\text{H}_2\text{O}_2$ -treated samples.



## **Identification of cytoprotective molecules using HCS**

### **Setting up a HCS method for screening cytoprotective molecules**

The HaCaT cell line was chosen as a model for screening because PARP-1-mediated cell death is well characterized in it. To detect cell death, the Sytox Green dye was chosen that is suitable for measuring cell membrane permeability. The measurement was performed on an Opera Phenix High Content Screening System and the images were analysed with the Harmony software. Several H<sub>2</sub>O<sub>2</sub> concentrations and time points were tested to adjust the experimental conditions. Treatment with 200 µM H<sub>2</sub>O<sub>2</sub> for 8 hours was found to be the most appropriate for screening. An FDA-approved molecule library in 10 96-well plates was tested in the screening. The Z-factor was greater than 0.5 for each plate, which is an excellent value for HCS. Molecules with cytoprotectivity above 50% were defined as “hit” compounds. 7 out of 20 “hit” compound was kept for further analysis after reviewing the literature. Validation was performed in 3 replicates according to the conditions used for HCS. All 7 molecules proved to be cytoprotective.

### **Ciclopirox and apomorphine are PARP inhibitory molecules**

As we wanted to select PARP inhibitors, so we performed PAR immunofluorescence on the HaCaT cells treated with the compounds. Ciclopirox and apomorphine inhibited PARylation after 10 minutes of H<sub>2</sub>O<sub>2</sub> treatment. A PARP-1 chromatin binding assay was performed to determine whether these agents inhibit the PARP-1 enzyme itself or they inhibit the complex formation between PARP-1 and the DNA or they act proximal to the PARP activation. Certain PARP inhibitors, such as olaparib, trap PARP-1 at the site of DNA breakage and induce a stable PARP-1-DNA complex. HaCaT cells were pretreated with olaparib and PJ34 (the latter does not cause PARP-1 trapping) in combination with ciclopirox and apomorphine. After 60 minutes of H<sub>2</sub>O<sub>2</sub> treatment, PARP-1 chromatin binding was increased. This trapping was reduced by either ciclopirox or apomorphine. Olaparib further enhanced PARP-1 DNA binding during H<sub>2</sub>O<sub>2</sub> treatment, which was also reduced by the two agents. PJ34 did not affect PARP-1 chromatin binding. A laser microirradiation experiment was performed to determine whether the agents affect the binding of PARP-1 to chromatin or inhibit it by other mechanisms. The appearance of PARP-1 was monitored over time in the area of microirradiation, the agents did not affect the accumulation of PARP-1 so they did

not affect the interaction between PARP-1 and the DNA, but the ROS-induced DNA damage.

### **Ciclopirox and apomorphine inhibit H<sub>2</sub>O<sub>2</sub>-induced genotoxicity**

Both ciclopirox and apomorphine decreased the single strand DNA breaks (Comet assay) during H<sub>2</sub>O<sub>2</sub> treatment. dsDNA breaks were detected with  $\gamma$ H2AX immunofluorescence. Nuclei were classified into three subpopulations: normal, damaged and highly damaged. There was a high proportion of the damaged population during the early stages of H<sub>2</sub>O<sub>2</sub> treatment and the highly damaged population appeared later. Ciclopirox and apomorphine significantly reduced the proportion of damaged and highly damaged populations. Based on the comet assay and the microscope images, we can say that these two agents protect against H<sub>2</sub>O<sub>2</sub> induced genotoxicity.

### **Ciclopirox and apomorphine act as Fe<sup>2+</sup> chelators**

We were able to characterize both agents through the phenotyping of cell death and describe the mechanism of PARP-1 activation. A crucial step in H<sub>2</sub>O<sub>2</sub> induced cell death is hydroxyl radical formation by the Fenton reaction. The hydroxyl radicals are highly capable of damaging DNA, so the question arises, whether these agents exercise their protective action against H<sub>2</sub>O<sub>2</sub>-induced genotoxicity through inhibition of the Fenton chemistry. To clarify this, a calcein “dequenching” assay was performed. Upon H<sub>2</sub>O<sub>2</sub> treatment, the calcein fluorescence decreased rapidly, which was quenched by the agents.

## Discussion

### Role of PARP-1 in the development of resistance against oxidative stress in polarized macrophages

Activated macrophages are one of the major ROS/RNS producers in the body and protective mechanisms are needed for their survival. In our work, we examined the changes surviving their survival when they undergo polarization. M1 macrophages were resistant to  $H_2O_2$ , while their M2 counterparts were not. Permeabilization of the cell membrane indicated a necrotic type of cell death to be involved in their demise. During polarization, a significant decrease was observed in two key parthanatos molecules (AIF and PARP-1) at the mRNA level. PARP-1 also showed a decrease at the protein level upon an LPS stimulus. A decrease in the PARP-1 protein level has been described in confluent cell cultures and during muscle cell differentiation, which correlated with increased resistance to oxidative stress in these models. The mRNA levels of several antioxidant genes (Txnrd1, Prxd1, Gsr, Sod2) were also significantly increased. Decreased PARylation and retained  $NAD^+$  levels could be measured in M1 macrophages after  $H_2O_2$  treatment. The experiment was also performed on PARP-1 KO cells, and it confirmed that PARP-1 was responsible for the PARylation and the  $NAD^+$  depletion. The regulatory role of PARP-1 after  $H_2O_2$  treatment was further confirmed with a cell death assay. PARP-1 KO cells died with slower kinetics and LPS-pretreated cells were resistant. From this, we concluded that not only a PARP-1 decrease is required for the development of cell death resistance, but there should be another mechanism, such as the previously described increased antioxidant gene expression. Another key player in parthanatos is AIF, which translocates from the mitochondria to the nucleus. Our model failed to verify the presence of nuclear AIF. A condensation of the nucleus occurred upon  $H_2O_2$  treatment, which was prevented by LPS pretreatment. The mitochondria play a central role in the life of a cell. Through its crucial role in metabolism, it is able to regulate the sensitivity of cells in various stressful situations. Decreased oxidative phosphorylation and increased aerobic glycolysis were observed in M1 macrophages. Decreased mitochondrial activity and increased glycolysis (Warburg effect) increase the chemoresistance of tumor cells. This metabolic shift could help macrophages survive oxidative stress, since decreased mitochondrial activity reduces the chance of secondary ROS production. Overall, the development of  $H_2O_2$  resistance in M1 macrophages can be explained by a multi-step process.

Decreased PARP-1 expression and activation, increased levels of antioxidant enzymes, and decreased mitochondrial activity all contribute to the development of cell death resistance.

### **Identification of cytoprotective molecules by a HCS method**

PARP inhibitors may be potential drug candidates not only in the fight against tumors but also in cell death caused by oxidative stress. In our work, we developed a HCS method for screening cytoprotective molecules. Screening was performed on an FDA-approved molecular library in which 774 molecules were tested. Two molecules (ciclopirox and apomorphine) proved to be PARP inhibitors, so these two molecules were further investigated. Both molecules inhibited the binding of PARP-1 to DNA upon H<sub>2</sub>O<sub>2</sub> treatment, but did not affect microirradiation and MNNG-induced DNA breakage-induced PARP-1 binding. From this, we concluded that the induction of ROS-induced DNA damage could be inhibited by these agents. The rate of single-stranded and double-stranded DNA breaks were reduced by the two selected molecules confirming our hypothesis. Examining the iron chelating ability of the compounds ciclopirox and apomorphine, we found that both agents were able to bind intracellular free Fe<sup>2+</sup> molecules. We can say that we have successfully set up a HCS method for screening cytoprotective molecules and identified several potential drug molecules as a result of the screening. We have characterized the protective mechanisms of two molecules, ciclopirox and apomorphine, and we can say that by inhibiting the Fenton reaction, they exert their protective effect proximally from PARP activation. It may be worth considering to use of these two agents against oxidative stress in the future.

## **Conclusions**

### **Role of PARP-1 in the development of resistance against oxidative stress in polarized macrophages**

1. Macrophages pretreated with LPS are resistant to H<sub>2</sub>O<sub>2</sub>.
2. Increased expression of antioxidant and decreased expression of cell death genes in LPS-treated macrophages.
3. Decreased PARP activity and preserved NAD<sup>+</sup> levels in M1 macrophages during H<sub>2</sub>O<sub>2</sub> treatment.
4. AIF independent parthanatos during H<sub>2</sub>O<sub>2</sub> treatment.
5. M1 macrophages gain energy from aerobic glycolysis and show decreased mitochondrial activity.

### **Identification of cytoprotective molecules by HCS method**

1. A HCS method for screening cytoprotective compounds was set up.
2. 7 out of 20 hit compounds were still unknown cytoprotective compounds that we were able to validate.
3. Among the molecules tested, ciclopirox and apomorphine are PARP inhibitors.
4. Ciclopirox and apomorphine inhibit H<sub>2</sub>O<sub>2</sub> induced genotoxicity.
5. Ciclopirox and apomorphine are Fe<sup>2+</sup> chelators, thus inhibiting Fenton reaction-induced radical production.

## Summary

Poly-ADP ribosylation plays a central role in the regulation of oxidative stress-induced cell death. During oxidative stress, inflammation and tissue damage and organ dysfunction occur. A better understanding of these processes can help us treat diseases such as diabetes, atherosclerosis, or ischemia/reperfusion more effectively. The main sources of ROS and RNS molecules that cause oxidative stress are macrophages. To survive, they must adapt to an environment with a high ROS content. In our work, we explored the molecular mechanisms developed by inflammatory macrophages to this end. LPS pretreated macrophages were resistant to H<sub>2</sub>O<sub>2</sub> treatment. Three main mechanisms are responsible for the development of their resistance. By decreasing PARP-1 expression and activation, they are able to avoid a drastic decrease in NAD<sup>+</sup> levels and a metabolic catastrophe during H<sub>2</sub>O<sub>2</sub> treatment. Another mechanism of their survival is the increased expression of antioxidant genes. Finally, cells also adapt to oxidative stress through a metabolic change where mitochondrial activity decreases and aerobic glycolysis increases (Warburg effect).

Drug development is especially important in modern medicine. We aimed to identify cell protective molecules capable of reducing PARP-1-regulated necrosis. In the FDA-approved molecular library, 7 cytoprotective molecules were identified and validated by the HCS method. Ciclopirox and apomorphine were identified as PARP inhibitors. These two agents did not directly inhibit the PARP-1 enzyme, but prevented the development of DNA damage proximal to it. Both agents function as chelators and protect cells by inhibiting the Fe<sup>2+</sup>-catalysed Fenton reaction.

PARP-1 plays a central role in oxidative stress-induced diseases. By inhibiting cell death, it is therefore important to better understand the regulatory role of PARP-1 and to develop molecules capable of inhibiting the enzyme-regulated pathway. The development of PARP inhibitors seems to be a promising solution not only in the fight against tumors but also in the treatment of other pathological processes.

## List of publications



UNIVERSITY of  
DEBRECEN

UNIVERSITY AND NATIONAL LIBRARY  
UNIVERSITY OF DEBRECEN

H-4002 Egyetem tér 1, Debrecen

Phone: +3652/410-443, email: publikaciok@lib.unideb.hu

Registry number: DEENK/82/2021.PL  
Subject: PhD Publication List

Candidate: Zsolt Regdon  
Doctoral School: Doctoral School of Molecular Medicine

### List of publications related to the dissertation

1. **Regdon, Z.**, Demény, M. Á., Kovács, K., Hajnád, Z., Nagy-Pénzes, M., Bakondi, E., Kiss, A., Hegedűs, C., Virág, L.: High-Content Screening identifies inhibitors of oxidative stress-induced parthanatos: cytoprotective and anti-inflammatory effects of ciclopirox. *Br. J. Pharmacol.* 2021, 1-19, 2021.  
DOI: <http://dx.doi.org/10.1111/bph.15344>  
IF: 7.73 (2019)
2. **Regdon, Z.**, Robaszkiewicz, A., Kovács, K., Rygielska, Ż., Hegedűs, C., Bodoor, K., Szabó, É., Virág, L.: LPS protects macrophages from AIF-independent parthanatos by downregulation of PARP1 expression, induction of SOD2 expression, and a metabolic shift to aerobic glycolysis. *Free Radic. Biol. Med.* 131, 184-196, 2019.  
DOI: <http://dx.doi.org/10.1016/j.freeradbiomed.2018.11.034>  
IF: 6.17

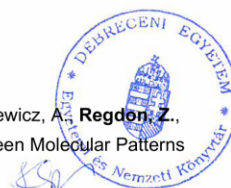
### List of other publications

3. Douida, A., Batista, F., Botó, P., **Regdon, Z.**, Robaszkiewicz, A., Tar, K.: Cells Lacking PA200 Adapt to Mitochondrial Dysfunction by Enhancing Glycolysis via Distinct Opa1 Processing. *Int. J. Mol. Sci.* 22 (4), 1-22, 2021.  
DOI: <http://dx.doi.org/10.3390/ijms22041629>  
IF: 4.556 (2019)
4. Kiss, A., Ráduly, A. P., **Regdon, Z.**, Polgár, Z., Tarapcsák, S., Sturniolo, I., El-Hamoly, T., Virág, L., Hegedűs, C.: Targeting nuclear NAD<sup>+</sup> synthesis inhibits DNA repair, impairs metabolic adaptation increases chemosensitivity of U-2OS osteosarcoma cells. *Cancers (Basel)*. 12 (5), 1-27, 2020.  
IF: 6.126 (2019)





5. Aladdin, A., Király, R., Botó, P., **Regdon, Z.**, Tar, K.: Juvenile Huntington's disease skin fibroblasts respond with elevated parkin level and increased proteasome activity as a potential mechanism to counterbalance the pathological consequences of mutant huntingtin protein. *Int. J. Mol. Sci.* 20 (5338), 1-39, 2019.  
IF: 4.556
6. Tokarz, P., Poszaj, T., **Regdon, Z.**, Virág, L., Robaszkiewicz, A.: PARP1-LSD1 functional interplay controls transcription of SOD2 that protects human pro-inflammatory macrophages from death under an oxidative condition. *Free Radic. Biol. Med.* 131, 218-224, 2019.  
DOI: <http://dx.doi.org/10.1016/j.freeradbiomed.2018.12.004>  
IF: 6.17
7. Virág, L., Jaén, R. I., **Regdon, Z.**, Boscá, L., Prieto, P.: Self-defense of macrophages against oxidative injury: fighting for their own survival. *Redox Biol.* 26, 1-9, 2019.  
DOI: <http://dx.doi.org/10.1016/j.redox.2019.101261>  
IF: 9.986
8. Bakondi, E., Singh, S. B., Hajnád, Z., Nagy-Pénzes, M., **Regdon, Z.**, Kovács, K., Hegedűs, C., Madácsy, T., Maléth, J., Hegyi, P., Demény, M. Á., Nagy, T., Kéki, S., Szabó, É., Virág, L.: Spilanthol Inhibits Inflammatory Transcription Factors and iNOS Expression in Macrophages and Exerts Anti-inflammatory Effects in Dermatitis and Pancreatitis. *Int. J. Mol. Sci.* 20 (17), 1-18, 2019.  
DOI: <http://dx.doi.org/10.3390/ijms20174308>  
IF: 4.556
9. Robaszkiewicz, A., Wisnik, E., **Regdon, Z.**, Chmielewska, K., Virág, L.: PARP1 facilitates EP300 recruitment to the promoters of the subset of RBL2-dependent genes. *Biochim. Biophys. Acta. Gene Regul. Mech.* 1861 (1), 41-53, 2018.  
DOI: <https://doi.org/10.1016/j.bbagr.2017.12.001>  
IF: 4.599
10. Hegedűs, C., Kovács, K., Polgár, Z., **Regdon, Z.**, Szabó, É., Robaszkiewicz, A., Forman, H. J., Martner, A., Virág, L.: Redox control of cancer cell destruction. *Redox Biol.* 16, 59-74, 2018.  
DOI: <http://dx.doi.org/10.1016/j.redox.2018.01.015>  
IF: 7.793
11. Bodnár, E., Bakondi, E., Kovács, K., Hegedűs, C., Lakatos, P., Robaszkiewicz, A., **Regdon, Z.**, Virág, L., Szabó, É.: Redox Profiling Reveals Clear Differences between Molecular Patterns of Wound Fluids from Acute and Chronic Wounds. *Oxid. Med. Cell. Longev.* 2018, 1-12, 2018.  
DOI: <http://dx.doi.org/10.1155/2018/5286785>  
IF: 4.868







12. Kovács, K., Erdélyi, K., Hegedűs, C., Lakatos, P., **Regdon, Z.**, Bai, P., Haskó, G., Szabó, É.,  
Virág, L.: Poly(ADP-ribosyl)ation is a survival mechanism in cigarette smoke-induced and  
hydrogen peroxide-mediated cell death.  
*Free Radic. Biol. Med.* 53 (9), 1680-1688, 2012.  
DOI: <http://dx.doi.org/10.1016/j.freeradbiomed.2012.08.579>  
IF: 5.271

**Total IF of journals (all publications): 72,381**

**Total IF of journals (publications related to the dissertation): 13,9**

The Candidate's publication data submitted to the iDEa Tudóstér have been validated by DEENK on  
the basis of the Journal Citation Report (Impact Factor) database.

08 March, 2021



The work was supported by National Research, Development and Innovation Office, and the GINOP-2.3.2-15-2016-00020 TUMORDNS, GINOP-2.3.2-15-2016-00048-STAYALIVE, and OTKA K132193 tenders.